Phosphatidic acid is required for the constitutive ruffling and macropinocytosis of phagocytes

Michal Bohdanowicz[a,*], Daniel Schlam[a,*], Martin Hermansson[b], David Rizzuti[a], Gregory D. Fairn[c], Takehiko Ueyama[d], Pentti Somerharju[b], Guangwei Du[e], and Sergio Grinstein[a,c]

[a]Division of Cell Biology, Hospital for Sick Children, Toronto, ON M5G 1X8, Canada; [b]Department of Biochemistry and Developmental Biology, University of Helsinki, Helsinki 00014, Finland; [c]Keenan Research Centre of the Li Ka Shing Knowledge Institute, St. Michael's Hospital, Toronto, ON M5C 1N8, Canada; [d]Laboratory of Molecular Pharmacology, Biosignal Research Center, Kobe University, Kobe 657-8501, Japan; [e]Department of Integrative Biology and Pharmacology, University of Texas Health Science Center at Houston, Houston, TX 77030

ABSTRACT **Macrophages and dendritic cells continuously survey their environment in search of foreign particles and soluble antigens. Such surveillance involves the ongoing extension of actin-rich protrusions and the consequent formation of phagosomes and macropinosomes. The signals inducing this constitutive cytoskeletal remodeling have not been defined. We report that, unlike nonphagocytic cells, macrophages and immature dendritic cells have elevated levels of phosphatidic acid (PA) in their plasma membrane. The plasmalemmal PA is synthesized by phosphorylation of diacylglycerol, which is in turn generated by a G protein–stimulated phospholipase C. Inhibition of diacylglycerol kinase activity results in the detachment of T-cell lymphoma invasion and metastasis–inducing protein 1 (TIAM1)—a Rac guanine exchange factor—from the plasma membrane, thereby depressing Rac activity and abolishing the constitutive ruffling and macropinocytosis that characterize macrophages and immature dendritic cells. Accumulation of PA and binding of TIAM1 to the membrane require the activity of phosphatidylinositol-4,5-bisphosphate 3-kinase. Thus a distinctive, constitutive pathway of PA biosynthesis promotes the actin remodeling required for immune surveillance.**

Monitoring Editor
Carole Parent
National Institutes of Health

Received: Nov 6, 2012
Revised: Mar 4, 2013
Accepted: Apr 1, 2013

INTRODUCTION

Macrophages and dendritic cells are professional phagocytes and antigen-presenting cells that provide immune surveillance and bridge the innate and adaptive immune systems. To this end, they constantly probe and sample the extracellular milieu for antigens. Particulate antigens are engulfed by phagocytosis, whereas soluble ones are internalized by macropinocytosis. Both processes are driven by actin polymerization initiated by activation of Rho-family GTPases. The membrane ruffling that underlies macropinosome formation occurs continuously and is particularly vigorous in immature dendritic cells (iDCs). Phagocytosis, by contrast, is believed to be a receptor-initiated process. However, evidence indicates that both macrophages and dendritic cells probe their surroundings for particulate targets by emitting extensions even before receptor engagement (West *et al.*, 2000; Flannagan *et al.*, 2010). Like phagocytosis itself, this spontaneous probing process is also actin mediated.

What triggers the ongoing extension of ruffles and filopodia in unstimulated phagocytes is not clear. We considered the possible involvement of phospholipids, which play a crucial role in controlling actin remodeling and undergo uniquely active conversions in phagocytic cells (Yeung and Grinstein, 2007). In particular, we investigated the role of phosphatidic acid (PA), which promotes actin polymerization by several means (Zhang and Du, 2009): it induces the dissociation of Rac from its Rho-specific guanine nucleotide dissociation inhibitor (GDI; Abramovici *et al.*, 2009), aids in recruiting Rac

This article was published online ahead of print in MBoC in Press (http://www.molbiolcell.org/cgi/doi/10.1091/mbc.E12-11-0789) on April 10, 2013.

*These authors contributed equally.

Address correspondence to: Sergio Grinstein (sergio.grinstein@sickkids.ca).

Abbreviations used: 2PABD, tandem phosphatidic acid–binding domain of Spo20p; CTB, *Clostridium difficile* toxin B; DAG, diacylglycerol; DGK, diacylglycerol kinase; DGKi I, diacylglycerol kinase inhibitor I; EtOH, ethanol; FIPI, 5-fluoro-2-indolyl deschlorohalopemide; GDI, guanine nucleotide dissociation inhibitor; GEF, guanine exchange factor; GPCR, G protein–coupled receptor; GPI, glycophosphatidylinositol; iDC, immature dendritic cells; PA, phosphatidic acid; PBD-PAK, p21-binding domain of p21-activated kinase; PI3K, phosphatidylinositol-4,5-bisphosphate 3-kinase; PKC, protein kinase C; PLC, phospholipase C; PLD, phospholipase D; PtdIns(4)P5K, phosphatidylinositol 4-phosphate 5-kinase; PtdIns(4,5)P_2, phosphatidylinositol 4,5-bisphosphate; TIAM1, T-cell lymphoma invasion and metastasis–inducing protein 1; TIRF, total internal reflection fluorescence.

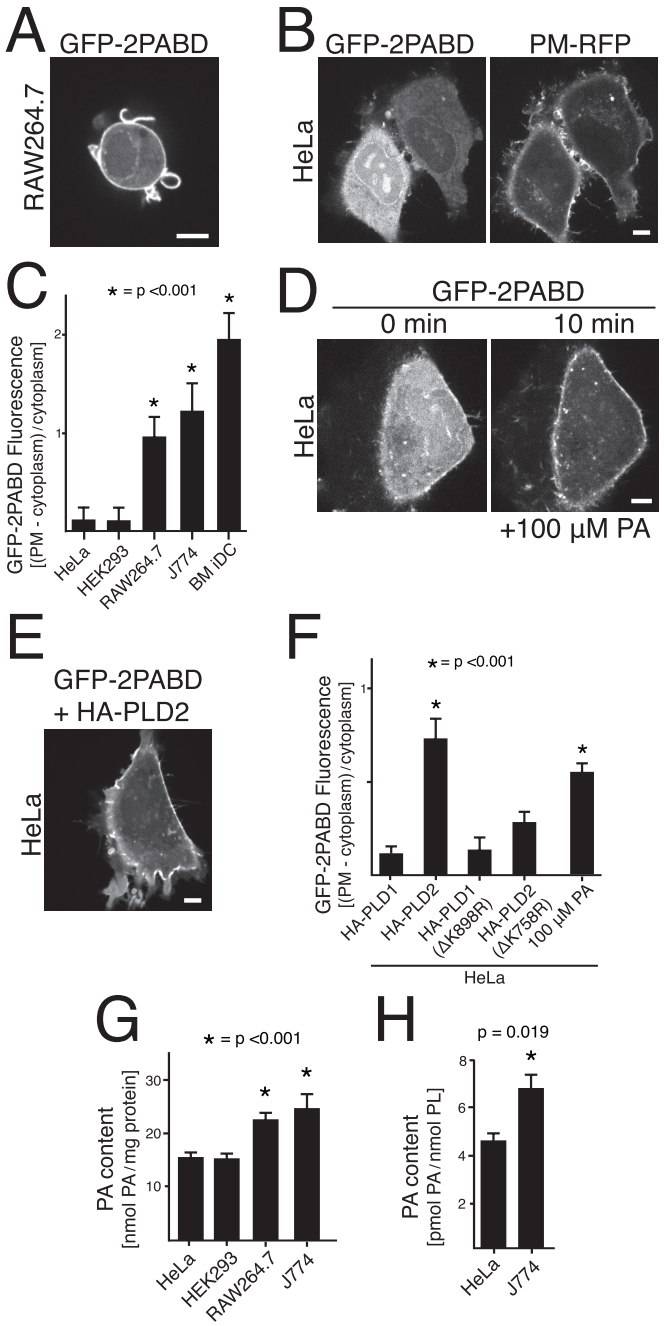

FIGURE 1: PA is elevated at the plasma membrane of macrophages and iDCs. (A) RAW264.7 macrophages transiently transfected with GFP-2PABD. A representative optical section obtained by confocal microscopy is illustrated. (B) HeLa cells transiently cotransfected with GFP-2PABD and PM-RFP were examined as in A. (C) Quantification of the fluorescence intensity of GFP-2PABD at the plasma membrane relative to that of the cytosol in various cell types. Data are means ± SE of at least three individual experiments; a minimum of 100 cells were quantified per cell type. (D) HeLa cells were transiently transfected with GFP-2PABD, and images were acquired before and 10 min after addition of exogenous PA. (E) Representative confocal fluorescence image of live HeLa cells transiently cotransfected with GFP-2PABD and HA-tagged PLD2. Scale bars, 5 µm. (F) Quantification of the fluorescence intensity of GFP-2PABD at the plasma membrane relative to that in the cytosol in HeLa cells transiently transfected with the indicated PLD constructs or exposed to 100 µM exogenous PA. Data are means ± SE of at least three individual experiments; a minimum of 100 cells were quantified per condition. (G) Quantification of the PA content of cell lysates, determined using the enzymatic assay described in *Materials and Methods*. Data are means ± SE of at least three individual experiments for each cell type. (H) Quantification of PA content of cell lysates by mass spectrometry. Data are means ± SE of at least three individual experiments.

to the plasma membrane (Stace and Ktistakis, 2006), and also activates the Rac guanine exchange factor (GEF), DOCK2 (Nishikimi *et al.*, 2009). In addition, PA contributes to the recruitment and activation of phosphatidylinositol 4-phosphate 5-kinase (PtdIns(4)P5K; Roach *et al.*, 2012); phosphatidylinositol 4,5-bisphosphate (PtdIns(4,5)P_2), the product of this kinase, facilitates actin polymerization by increasing the concentration of monomeric actin and controlling the severing of filaments (Zhang *et al.*, 2012).

Although genetically encoded fluorescent probes have been used successfully to monitor the dynamics of other phospholipids, detection of PA in live cells has been uniquely challenging, perhaps because it is a minor, rapidly interconvertible species. A probe based on the PA-binding domain of Raf1 has been used with some success (Rizzo *et al.*, 2000) but appears to lack the sensitivity needed to detect low levels of the phospholipid. Another protein domain, identified in the yeast protein Spo20p, also binds PA selectively (Nakanishi *et al.*, 2004; Kassas *et al.*, 2012). Here we use a construct consisting of two tandem repeats of the Spo20p domain fused to a nuclear export signal to visualize PA in macrophages and iDCs. Microscopy studies performed using this probe, in combination with mass spectrometry and enzymatic determinations, reveal that phagocytes are uniquely rich in plasmalemmal PA. Phosphorylation of diacylglycerol (DAG) by DAG kinase(s) (DGKs) is primarily responsible for the formation of this basal PA, which is necessary for the constitutive ruffling that underlies macropinocytosis.

RESULTS

Plasmalemmal PA in macrophages and iDCs

We used a tandem repeat of the Spo20p$^{51–91}$ domain fused to green fluorescent protein (GFP) as a genetically encoded probe for PA (Zeniou-Meyer *et al.*, 2007; Du and Frohman, 2009; see *Materials and Methods*). When expressed in macrophage-like RAW264.7 or J774 cells, the probe (called GFP–tandem phosphatidic acid–binding domain of Spo20p [2PABD] hereafter) associates with the plasma membrane (Figure 1A), implying that PA is particularly abundant in this compartment; this conclusion is in agreement with mass spectrometric determinations in RAW264.7 cells (Andreyev *et al.*, 2010). A smaller fraction of the probe bound the nuclear/endoplasmic reticulum (ER) membrane, where PA serves as a precursor for glycerophospholipid synthesis. Of importance, the plasmalemmal enrichment of PA occurred also in primary myeloid cells. This was verified by introducing the plasmid encoding GFP-2PABD into bone marrow–derived murine iDCs by electroporation. In keeping with the findings using cell lines, the PA probe was found overwhelmingly at the plasma membrane (Figure 1C and Supplemental Movie S1). By contrast, in nonphagocytic cells such as epithelioid HeLa or kidney-derived HEK293 cells, PA localized to the nuclear/ER membrane and inside the nucleus, but the majority was cytosolic (Figure 1B). Of note, little PA was detected at the plasma membrane, which was demarcated using a plasmalemmal marker, PM–red fluorescent protein (RFP; Figure 1C). The failure of the probe to bind to the plasmalemma in HeLa and HEK293 cells reflects the scarcity of PA in this compartment rather than abnormal behavior of the probe in these cells. This was validated by addition of exogenous PA, which partitioned into the plasma membrane and caused a rapid and extensive relocalization of the GFP-2PABD construct to the plasmalemma

(Figure 1, D and F). Moreover, the probe could readily detect metabolically generated PA at the membrane of HeLa cells, as shown in Figure 1E. For these experiments, cells were transfected with phospholipase D2 (PLD2), which localizes to the plasma membrane, where it displays high basal activity; expression of this isoform recruited the PA probe to the membrane. This effect was not observed when a catalytically inactive mutant was transfected (Figure 1F). Moreover, the distribution of the probe remained similarly unaffected when PLD1 was expressed. Unlike PLD2, this isoform is found mainly in endocytic and Golgi compartments and is relatively inactive at rest (Du *et al.*, 2003).

PA is an essential precursor for glycerophospholipid and triglyceride synthesis that occur in endomembranes (Bohdanowicz and Grinstein, 2013). Because phagocytes displayed unusually high PA at the plasma membrane, in addition to the fraction detected in endomembranes, we predicted that their total PA content per cell would be higher than that of nonmyeloid cells. Two methods were used to test this prediction: mass spectrometry and an enzymatic assay in which PA is metabolized to generate a fluorescent product (see *Materials and Methods*; Morita *et al.*, 2009). As illustrated in Figure 1G, the latter assay indicated that, when normalized per unit protein, macrophage-like cells indeed contain considerably more PA than do nonmyeloid cells. Furthermore, we also quantified PA by mass spectrometry. These determinations confirmed that the total PA—expressed per total phospholipid—was greater in phagocytic than in nonphagocytic cells (Figure 1H).

Plasmalemmal PA is produced by DGK

PLD activity is an acknowledged source of PA (Yeung and Grinstein, 2007). We therefore assessed its contribution to the pool of PA present constitutively in the membrane of phagocytes. Neither 1-butanol nor 5-fluoro-2-indolyl des-chlorohalopemide (FIPI), two well-documented antagonists of PLD-mediated PA production, had a significant effect on the membrane partition of the GFP-2PABD probe (Figure 2, A and B), and neither compound decreased the total content of PA, as measured using the aforementioned enzymatic assay (Figure 2C). The effectiveness of the inhibitors was verified using HeLa cells transfected with PLD2; in this instance, both 1-butanol and FIPI displaced the GFP-2PABD probe from the plasma membrane (Figure 2, D and E). Furthermore, the catalytically inactive mutants of PLD1 and PLD2, which are often used as dominant-negative antagonists of endogenous PLD, failed to decrease the plasmalemmal PA in RAW264.7 cells (Figure 2B).

The preceding results suggest that a pathway other than PLD is responsible for PA formation in the membrane of phagocytes. We next tested the role of DGKs, which catalyze the phosphorylation of DAG into PA. In stark contrast to PLD antagonists, diacylglycerol kinase inhibitor I (DGKi I; also called R59022) prompted dissociation of the PA probe from the plasma membrane of RAW264.7 cells (Figure 2F) and myeloid cells (Supplemental Movie S1). The probe detached rapidly from the membrane after addition of DGKi I, with a half-life of ~80 s (Figure 2G), implying rapid turnover of PA. Ethanol, the vehicle used to dissolve DGKi I, was without effect. Two lines of evidence indicate that the inhibitor indeed precluded DGK activity rather than interfered by other means with the binding of the PA probe. First, in parallel with the decrease in PA, DGKi I caused plasmalemmal accumulation of DAG, monitored using the C1 domain of protein kinase Cδ (Figure 2F, bottom). Second, addition of exogenous PA to cells treated with DGKi I restored binding of GFP-2PABD to the membrane (Figure 2H). Moreover, as shown in Figure 2C, DGKi I also reduced the total PA content of the cells by 54%, measured biochemically. Taken together, these results suggest that DGK activity is the predominant source of constitutive plasmalemmal PA production in phagocytes.

Expression and localization of DGK isoforms

Ten different members of the DGK family have been described (Sakane *et al.*, 2007). We tested whether one or more of these are expressed in macrophages and whether they localize to the plasma membrane. Strikingly, using reverse transcription (RT)-PCR, we found that all 10 DGKs are present in RAW264.7 macrophages (Figure 3A). Expression of GFP-tagged versions of the DGKs was used to assess their subcellular distribution. Of the six GFP-tagged DGKs tested, DGKβ, DGKγ, and DGKζ were found at the plasma membrane of otherwise untreated RAW264.7 cells (Figure 3, B–E). The expression and localization of multiple DGK isoforms support the hypothesis that these enzymes are responsible for plasmalemmal PA production.

PA production depends on phospholipase C activity

The rapid accumulation of DAG in cells treated with DGKi I suggests that ongoing DAG generation is obscured by its rapid conversion to PA by DGK. Because at rest the concentration of plasmalemmal PA remains constant, this implies that PA synthesis is matched by its conversion to further products. If such a dynamic steady state indeed exists, it follows that inhibition of DAG production should result in a concomitant depletion of PA. Indeed, inhibition of phospholipase C (PLC), which is most commonly responsible for DAG production at the plasma membrane, by the PLC inhibitor U73122 decreased the PA content of RAW264.7 cells (Figure 4A). Using the converse approach—addition of the PLC activator ionomycin to HeLa cells—caused a transient accumulation of the PA probe at the plasma membrane (Figure 4, B and C, and Supplemental Movie S2).

Thirteen PLC family members have been identified (Bunney and Katan, 2011). Their potential redundancy made identification of the responsible enzyme(s) by small interfering RNA–mediated silencing impractical. Instead we investigated whether any of the isoforms were located at the plasma membrane in resting macrophages. PLCγ1 and PLCγ2, which play an important role during phagocytosis, were not localized to the plasma membrane under unstimulated conditions: PLCγ1-GFP and PLCγ2-GFP were largely cytosolic, and immunofluorescence determinations similarly failed to detect endogenous PLCγ1 or PLCγ2 at the membrane (Supplemental Figure S1). We next tested PLCβ isoforms. PLCβ1-GFP and PLCβ3–cyan fluorescent protein (CFP) were present in the plasma membrane of RAW264.7 macrophages (Figure 4, D and E), and RT-PCR suggested that messages for both enzymes are generated by these cells (Figure 4F). Moreover, PLCβ3 has been reported to regulate macrophage survival (Wang *et al.*, 2008).

Activation of PLC and PtdIns(4,5)P_2 3-kinase by G protein–coupled receptors is required for synthesis of plasmalemmal PA in phagocytes

To analyze the possible involvement of PLCβ in DAG and PA generation, we took advantage of the fact that these isoforms are stimulated by G protein–coupled receptors (GPCRs). To this end, we used pertussis toxin (PTX), which blocks Gi, Go, and Gt proteins from coupling with their cognate receptors. As illustrated in Figure 5D, PTX lowered the total PA content of RAW264.7 cells and caused the PA probe to dissociate from the plasma membrane (Figure 5, E and F). Furthermore, PTX caused detachment of PLCβ3-CFP from the plasma membrane (Figure 5F). We also tested the effect of an activator of GPCRs. Addition of aluminum fluoride to HeLa cells caused accumulation of plasmalemmal DAG that was accompanied by

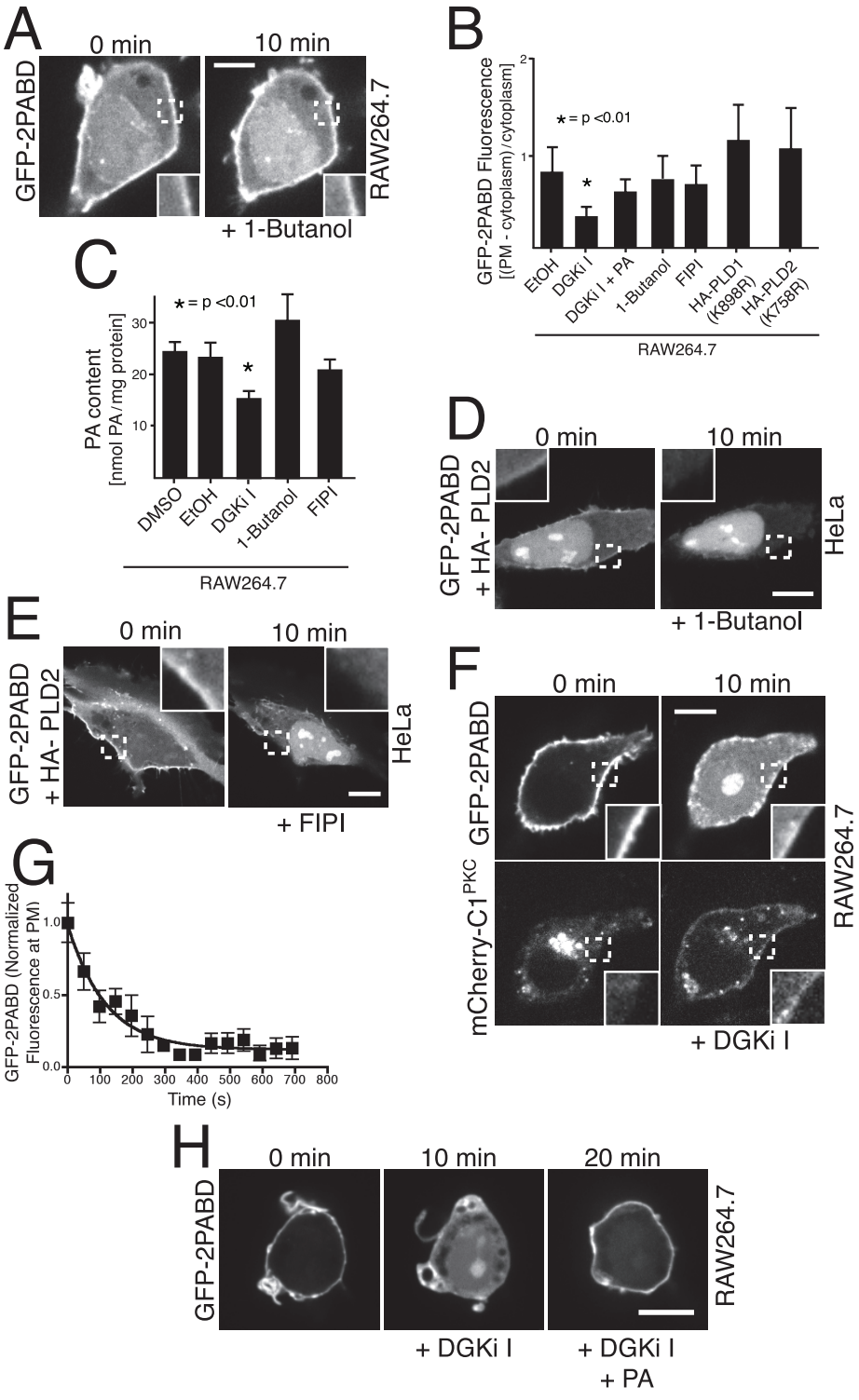

FIGURE 2: Plasmalemmal PA is generated by DGK. (A) RAW264.7 macrophages transiently transfected with GFP-2PABD or (D, E) HeLa cells cotransfected with GFP-2PABD and HA-PLD2 were examined by confocal microscopy immediately before and 10 min after treatment with (A, D) 0.3% 1-butanol or (E) 750 nM FIPI. Insets here and elsewhere show magnifications of the area denoted by the dashed line. (B) Quantification of the fluorescence intensity of GFP-2PABD at the plasma membrane of RAW264.7 macrophages relative to that of the cytosol. Data are means ± SE of at least three individual experiments; a minimum of 50 cells were quantified per condition. (C) Quantification of the PA content of RAW264.7 cell lysates using the enzymatic assay. Data are means ± SE of at least three individual experiments. (F) RAW264.7 macrophages cotransfected with GFP-2PABD and mCherry-C1^{PKC} were examined by confocal microscopy before or 10 min after treatment with 30 μM DGKi I. (G) Quantitation of the fluorescence intensity of GFP-2PABD at the plasma membrane of RAW264.7 macrophages as a function of time after exposure to 30 μM DGKi I. Plasmalemmal fluorescence was normalized to the initial value to enable comparison between experiments. Data are means ± SEM of six independent determinations. (H) RAW264.7 macrophages transfected with GFP-2PABD were examined by confocal microscopy before, 10 min after treatment with 30 μM DGKi I, and a further 10 min after the subsequent addition of 100 μM PA. Images in A, D, F, and H are representative of at least three experiments of each kind. Scale bars, 5 μm.

recruitment of the PA probe (Figure 5, B and C, and Supplemental Movie S3).

The pronounced effect of PTX on plasmalemmal PA biosynthesis, as well as the sensitivity of PLCβ isoforms to this toxin, led us to question whether other key lipid intermediates upstream of PA synthesis were also affected by PTX treatment. We therefore examined the distribution of DAG (the substrate of DGKs), PtdIns(4,5)P_2 (the primary substrate of PLCβ), and PtdIns(3,4,5)P_3 (which regulates the targeting and activity of PLC isoforms), using fluorescently tagged biosensors. As shown in Figure 5E, exposure to PTX had no discernible effect on the cellular localization of PH-PLCδ-GFP and GFP-C1^{PKC} (PKC, protein kinase C) sensors for PtdIns(4,5)P_2 and DAG, respectively. In contrast, the toxin caused dissociation of PH-Akt-GFP (a probe for PtdIns(3,4,5)P_3) from the plasma membrane, where it was found to be enriched in ruffles. Modest amounts of PtdIns(3,4,5)P_3 had been detected earlier in the membrane of unstimulated macrophages, which increase markedly during phagocytosis (Vieira *et al.*, 2001).

The shared sensitivity of PA and PtdIns(3,4,5)P_3 formation to PTX raised the possibility that these events might be causally linked. Indeed, PtdIns(3,4,5)P_3 was shown to target to the membrane and stimulate the activity of a variety of PLC isoforms, including PLCβ3 (Zhang *et al.*, 2009). We therefore used phosphatidylinositol-4,5-bisphosphate 3-kinase (PI3K) inhibitors to test whether PtdIns(3,4,5)P_3 is in fact required for the constitutive accumulation of PA at the plasma membrane of phagocytes. We verified the effectiveness of the PI3K inhibitor LY294002 by measuring the displacement of the PX domain of p40^{phox} (a probe for PtdIns(3)P) from endomembranes (Figure 5A). In parallel with inhibition of PI3K activity, LY294002 caused detachment of the PA probe GFP-2PABD from the plasma membrane. Addition of exogenous PA restored plasmalemmal localization of GFP-2PABD to

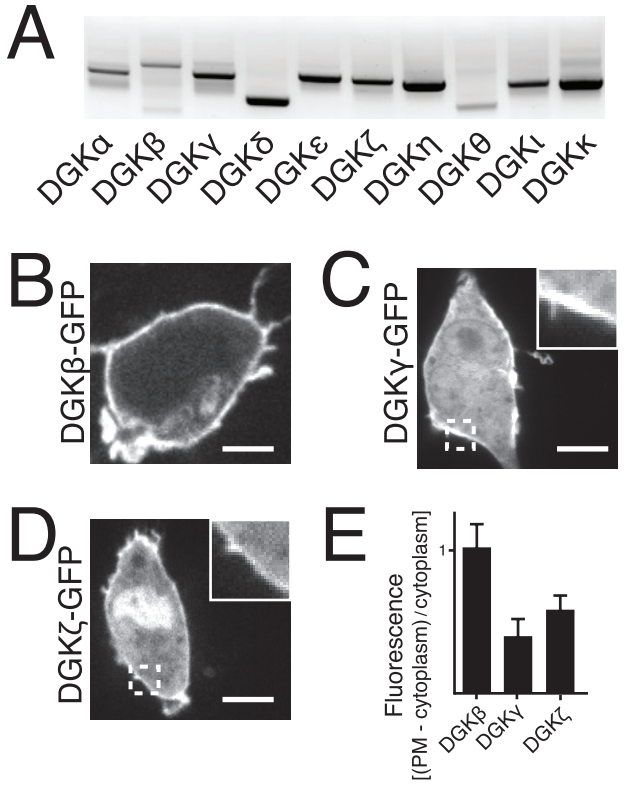

FIGURE 3: Expression of DGK isoforms in macrophages. (A) Transcription of all 10 DGK isoforms was validated by RT-PCR using mRNA extracted from RAW264.7 macrophages. (B–D) RAW264.7 macrophages were transiently transfected with (B) DGKβ-GFP, (C) DGKγ-GFP, or (D) DGKζ-GFP and examined by confocal microscopy. Scale bars, 5 μm. (E) Quantification of fluorescence of the different DGK isoforms at the plasma membrane relative to that in the cytosol. Data are means ± SE of at least three individual experiments; a minimum of 100 cells were quantified per condition.

the membrane, implying that LY294002 does not directly interfere with the ability of the probe to recognize PA (Figure 5A, bottom). This finding also implies that the GFP-2PABD probe does not require PtdIns(3,4,5)P_3 to associate with the membrane. Accordingly, by stimulating PI3K, insulin recruits PH-Akt-RFP, but not GFP-2PABD, to the plasma membrane of HeLa cells (Supplemental Figure S2A). Conversely, DGKi I causes GFP-2PABD, but not PH-Akt-RFP, to dissociate from the plasma membrane of RAW264.7 cells (Supplemental Figure S2B). Taken together, these findings indicate that the novel GFP-2PABD probe recognizes PA but not PtdIns(3,4,5)P_3.

The preceding observations support the notion that constitutive production of PA at the plasma membrane depends on the activity of PI3K and PLCβ, both of which are in turn regulated by PTX-sensitive G proteins. Although these results provide convincing evidence of the involvement of PTX-sensitive GPCRs, we were unable to pinpoint the precise receptor(s) involved. Inhibitors of sphingosine 1-phosphate, lysophosphatidic acid, prostaglandin, or P2Y receptors were without effect on the membrane association of the GFP-2PABD probe (data not shown). Similarly, serum starvation for 6 h had no discernible effect, and we could not detect autocrine or paracrine factors by incubating HeLa cells with conditioned medium used to culture RAW264.7 cells. It is possible that more than one GPCR or an orphan GPCR stimulates plasmalemmal DAG and PA production in phagocytic cells.

PA production depends on PtdIns(4,5)P_2

PtdIns(4,5)P_2 is the preferred substrate of most mammalian PLCs. To determine whether PtdIns(4,5)P_2 was required for plasmalemmal PA production, we used a rapamycin heterodimerization system to recruit to the plasma membrane the phosphatase domain of synaptojanin, which can hydrolyze PtdIns(4,5)P_2. The system consists of two separate constructs. One is soluble and includes both the phosphatase and rapamycin-binding domains. The second construct is associated with the plasmalemma and binds to another moiety of rapamycin. Addition of rapamycin brings the phosphatase to the membrane by promoting the complementary interaction between rapamycin-binding domains in the cytosolic and plasmalemmal constructs (Figure 6A). As shown in Figure 6, B and D, recruitment of the phosphatase caused dissociation of the GFP-2PABD from the membrane, indicating that the continuous formation of PA required the presence of PtdIns(4,5)P_2. That the effect of rapamycin was due to depletion of PtdIns(4,5)P_2 was confirmed by using a catalytically inactive mutant of the phosphatase. Rapamycin-induced recruitment of this mutant had no discernible effect on PA (Figure 6, C and D).

PA is necessary for the plasmalemmal Rac activity that underlies membrane ruffling

PA can regulate Rac activity (Abramovici *et al.*, 2009; Nishikimi *et al.*, 2009), a monomeric GTPase key to membrane ruffle formation (West *et al.*, 2000; Flannagan *et al.*, 2010). It seemed plausible that PA was involved in the constitutive ruffling that macrophages and iDCs undergo in the course of immune surveillance. Indeed, plasmalemmal PA abundance closely parallels ruffling, as RAW264.7 and iDCs—which have more PA—ruffle much more actively than HeLa cells (Supplemental Movie S4). We therefore tested how membrane ruffling was affected when PA production was impaired. Inhibition of DGK activity depressed both the rate and extent of ruffle formation in iDCs (Figure 7, A and B). The ruffling index in these cells, measured as in Araki *et al.* (1996), decreased by 65%, and this was accompanied by a decrease in the actin-rich frilled protrusions believed to underlie ruffle formation (Figure 7C). Note that the total F-actin content of the cells—measured by extracting bound phalloidin with methanol—was unaffected by the DGK inhibitor (Supplemental Figure S3A), indicating that its effect was specifically on ruffling and not a wholesale inhibition of actin polymerization. Indeed, some RAW264.7 cells treated with the DGK inhibitor exhibited bundles of actin reminiscent of stress fibers (Supplemental Figure S3B), suggesting an alteration of the equilibrium between Rho and Rac activity.

We confirmed and extended the ruffling index and phalloidin determinations using an independent method based on total internal reflection fluorescence (TIRF) microscopy. RAW264.7 cells stably expressing glycophosphatidylinositol-anchored GFP, an exofacial marker, were suspended and allowed to settle onto a coverslip coated with bovine serum albumin (for details see Flannagan *et al.*, 2010). Once the cells made contact with the coverslip, dynamic membrane protrusions were readily visible in the focal (TIRF) plane (Figure 7D and Supplemental Movie S5). Integration of the fluorescence over time provided a robust measure of ruffling activity. As expected, when quantified in this manner, ruffling was inhibited by latrunculin B, an actin-polymerization antagonist. More important, profound inhibition was also recorded in cells treated with DGKi I or PTX (Figure 7, D and E).

We verified that the inhibition of ruffling was caused by interference with Rac, using a construct consisting of the p21-binding domain of p21-activated kinase (PBD-PAK) tagged with yellow fluorescent protein (YFP). PAK-PBD-YFP is used routinely as an indicator of

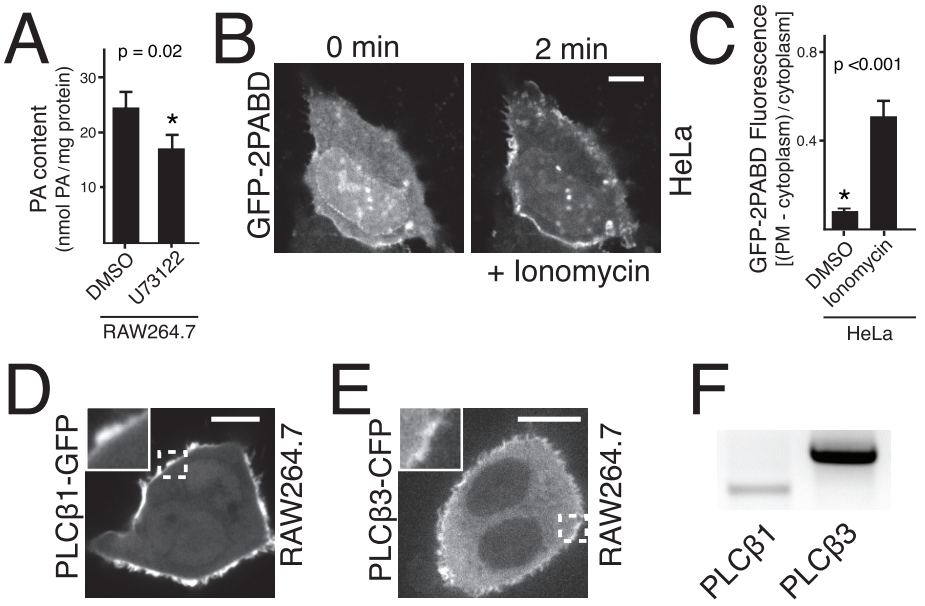

FIGURE 4: PLC isoforms localize to the plasma membrane of macrophages, where they catalyze formation of intermediates of PA biosynthesis. (A) Quantification of PA content of RAW264.7 macrophage lysates using the enzymatic assay. Cells were pretreated with 2 μM of the PLC inhibitor U73122 for 20 min or with vehicle (dimethyl sulfoxide [DMSO]) alone. Data are means ± SE of at least three individual experiments. (B) HeLa cells transiently transfected with GFP-2PABD and treated with ionomycin were imaged by confocal microscopy. Scale bar, 5 μm. (C) Quantification of fluorescence at the plasma membrane of HeLa cells transiently transfected with GFP-2PABD and treated with DMSO alone or with 1 μM ionomycin for 2 min. Data are means ± SE of at least three individual experiments; a minimum of 20 cells were quantified per condition. (D, E) RAW264.7 macrophages were transiently transfected with (D) PLCβ1-GFP or (E) PLCβ3-CFP and imaged by confocal microscopy. (F) RT-PCR of PLCβ1 and β3 using mRNA from RAW264.7 macrophages.

Rac activity (Srinivasan *et al.*, 2003). When expressed in RAW264.7 cells, the construct accumulated in ruffles that formed spontaneously, consistent with Rac involvement (Figure 7G). Incubation with DGKi I reduced the number of PAK-PBD-YFP–enriched ruffles. PAK-PBD-YFP also weakly associates with active Cdc42 (Srinivasan *et al.*, 2003). To ensure that Rac was in fact the target of modulation by PA, we also used an enzyme-linked immunosorbent assay that detects Rac activity specifically (Figure 7F). Unstimulated macrophages displayed readily detectable Rac activity that, as expected, was virtually eliminated by *Clostridium difficile* toxin B (CTB). Of importance, this resting activity was also markedly depressed by DGKi I. That Rac deactivation is accompanied by a decrease in plasmalemmal PA was verified by transiently cotransfecting constructs encoding PAK-PBD-YFP and GFP-PABD before exposure of the cells to PTX. As demonstrated in Figure 7H, PTX impaired membrane ruffling and led to displacement of PAK-PBD-YFP and GFP-2PABD form the plasma membrane. Whereas addition of exogenous PA rescued the association of GFP-2PABD with the plasma membrane, this treatment was not sufficient to reactivate Rac or to induce de novo formation of membrane ruffles (Supplemental Movie S6), indicating that PA signaling is necessary but not sufficient to support activation of plasmalemmal Rac. Other, factors, likely including PtdIns(3,4,5)P_3, are necessary to support Rac activation and constitutive ruffling.

Association of the Rac nucleotide-exchange factor, T-cell lymphoma invasion and metastasis–inducing protein 1, with the plasma membrane; role of PA and PtdIns(3,4,5)P_3

PA was recently reported to promote the recruitment of DOCK2, a Rac-GEF, by interacting with a polybasic region at its C-terminal end (Nishikimi *et al.*, 2009). Another GEF, T-cell lymphoma invasion and metastasis–inducing protein 1 (TIAM1), was identified as an important activator of Rac in macrophages (Mizrahi *et al.*, 2005). Like DOCK2, TIAM1 contains a polybasic domain, consisting of five consecutive arginines, near its C-terminus. We therefore investigated whether PA contributes to its association with the membrane. As shown in Figure 8A, the GFP-tagged version of TIAM1 constitutively localizes to the plasma membrane of macrophages and is particularly noticeable at ruffles. Addition of the DGK inhibitor caused this Rac GEF to detach from the membrane while concomitantly terminating ruffling (Figure 8, A and C, and Supplemental Movie S7). Addition of exogenous PA rerecruited TIAM1-GFP to the membrane and restored ruffling (Supplemental Movie S7, B). In contrast, addition of exogenous DAG to DGKi I–treated cells was unable to relocate TIAM1-GFP to the membrane (Figure 8C and Supplemental Movie S7, A). The inhibitory effect of DGKi I on TIAM1 was not due to a global effect on plasmalemmal surface charge, as indicated by the retention on the membrane of the cationic probe GFP-R-pre, described earlier (Yeung *et al.*, 2006; Supplemental Figure S4). These findings indicate that not only DOCK2, but also TIAM1 could account for the constitutive, PA-dependent activity of Rac on the membrane of phagocytes.

Whereas addition of exogenous PA was sufficient to restore plasmalemmal association of TIAM1 and membrane ruffling (Figure 8, A and C, and Supplemental Movie S7) in cells treated with DGKi I, it was insufficient to restore ruffling in cells exposed to PTX (Figure 7H and Supplemental Movie S6). Thus, although it is clear that PA is necessary for the association of TIAM1 with the plasma membrane, PTX seemingly interferes also with other components necessary for constitutive recruitment of TIAM1. Because PTX treatment led to a marked decrease in plasmalemmal PtdIns(3,4,5)P_3 (Figure 5, E and F), we considered the possibility that this inositide was also required for the recruitment of TIAM1 to the plasma membrane (Ceccarelli *et al.*, 2007). We therefore treated RAW264.7 macrophages coexpressing TIAM1-GFP and PX-mCherry with LY294002. As found when using the DAG kinase inhibitor (Figure 8A), PI3K inhibition resulted in the displacement of TIAM1-GFP from the plasma membrane (Figure 8, B and C). Of importance, inhibition of PI3K resulted in the concomitant impairment of membrane ruffling (Supplemental Movie S8). Taken together, these results imply that plasmalemmal PA and PtdIns(3,4,5)P_3 need to be present simultaneously for optimal recruitment of TIAM1.

The parallel behavior of TIAM1 and cell ruffling suggests that nucleotide exchange by Rac is the main determinant of actin remodeling under the conditions analyzed in the foregoing. If this is indeed the case, then expression of a recombinant exchange factor that permanently associates with the plasma membrane should bypass the requirement for PI3K and DGK signaling. To test this hypothesis, we expressed the GEF (tandem DH-PH) domain of TIAM1 joined by a flexible linker to the rapamycin-binding domain FKBP (Inoue *et al.*, 2005), tagged with enhanced YFP. A diagrammatic representation of

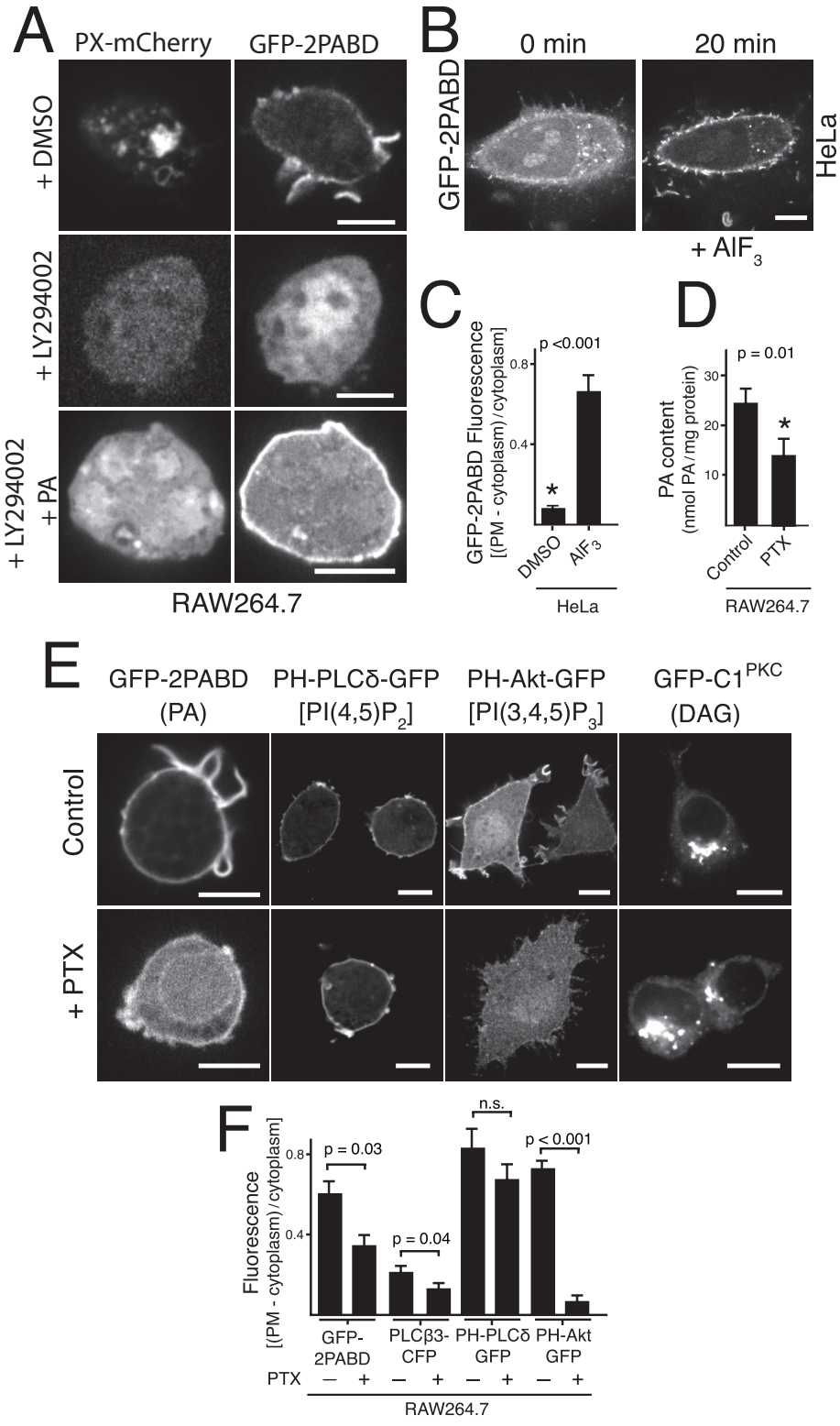

FIGURE 5: GPCR signaling and PI3K activity are required for synthesis of plasmalemmal PA in macrophages. (A) RAW264.7 macrophages were transiently cotransfected with constructs encoding GFP-2PABD, as well as PX-mCherry, a PtdIns(3)P fluorescent biosensor to monitor PI3K activity, and examined by confocal microscopy. Macrophages were treated with solvent only (DMSO; top), 100 μM LY294002 alone (middle), or LY294002 followed by addition of exogenous PA (bottom). (B) HeLa cells were transfected with GFP-2PABD and examined immediately before and 20 min after treatment with 50 μM aluminum fluoride. (C) Quantification of plasmalemmal fluorescence for experiments depicted in B. (D) Quantification of the PA content in RAW264.7 cell lysates before and after exposure to PTX. Data in C and D are means ± SE of at least three individual experiments; a minimum of 50 cells were quantified per condition. (E) RAW264.7 macrophages were transfected with GFP chimeric constructs encoding 2PABD, the PH domain of PLCδ (a probe for PtdIns(4,5)P_2,), the PH domain of Akt (a probe for PtdIns(3,4,5)P_3 and PtdIns(3,4)P_2), or the C1 domain of PKCδ, a probe for DAG. The distribution of the corresponding lipids was monitored by confocal microscopy in otherwise untreated (Control; top) cells and in cells exposed to PTX for 16 h (bottom). Scale bars, 5 μm. (F) Quantification of plasma membrane fluorescence of RAW264.7 cells transfected with the lipid biosensors or with PLCβ3-CFP. Where indicated, cells were pretreated with 0.1 μg/ml PTX for 16 h. Data are means of at least three individual experiments; a minimum of 30 cells were quantified per condition.

this construct (hereafter referred to as YF-TIAM1) is shown in Figure 8D, where it is compared with the full-length TIAM1-GFP. The YF-TIAM1 construct was cotransfected with LDR, its heterodimerization partner, which is targeted to the plasma membrane. In the absence of the dimerizing agent rapamycin, YF-TIAM1 was entirely cytosolic (Figure 8E). However, upon addition of rapamycin, YF-TIAM1 translocated to the plasma membrane, where it induced the formation of extensive dorsal ruffles, in excess over those forming spontaneously. Most important, TIAM1 was recruited to phagocyte surfaces even when cells had been preincubated for 20 min with fully inhibitory doses of DGKi or LY294002, and this was accompanied by equally pronounced dorsal ruffling (Figure 8E). These data provide strong evidence that plasmalemmal association of TIAM1 (and/or other GEFs) is both necessary and sufficient to induce membrane ruffling in phagocytes.

PA is required for macropinocytosis

Membrane ruffling underlies macropinocytosis. We therefore anticipated that inhibition of PA synthesis would also impair macropinosome formation. We tested this prediction by treating the phagocytes with DGKi I. Under control conditions, iDCs internalized labeled dextran into large vacuoles, likely macropinosomes (Figure 9A). On DGK inhibition the amount of dextran internalized decreased markedly, and uptake was associated with smaller vesicles, presumably endosomes (Figure 9, A and B). Although less active than iDCs, resting RAW264.7 cells also formed macropinosomes spontaneously, and their formation was impaired by both DGKi I and the PLC inhibitor U73122 (Figure 9C). These observations support the notion that PA

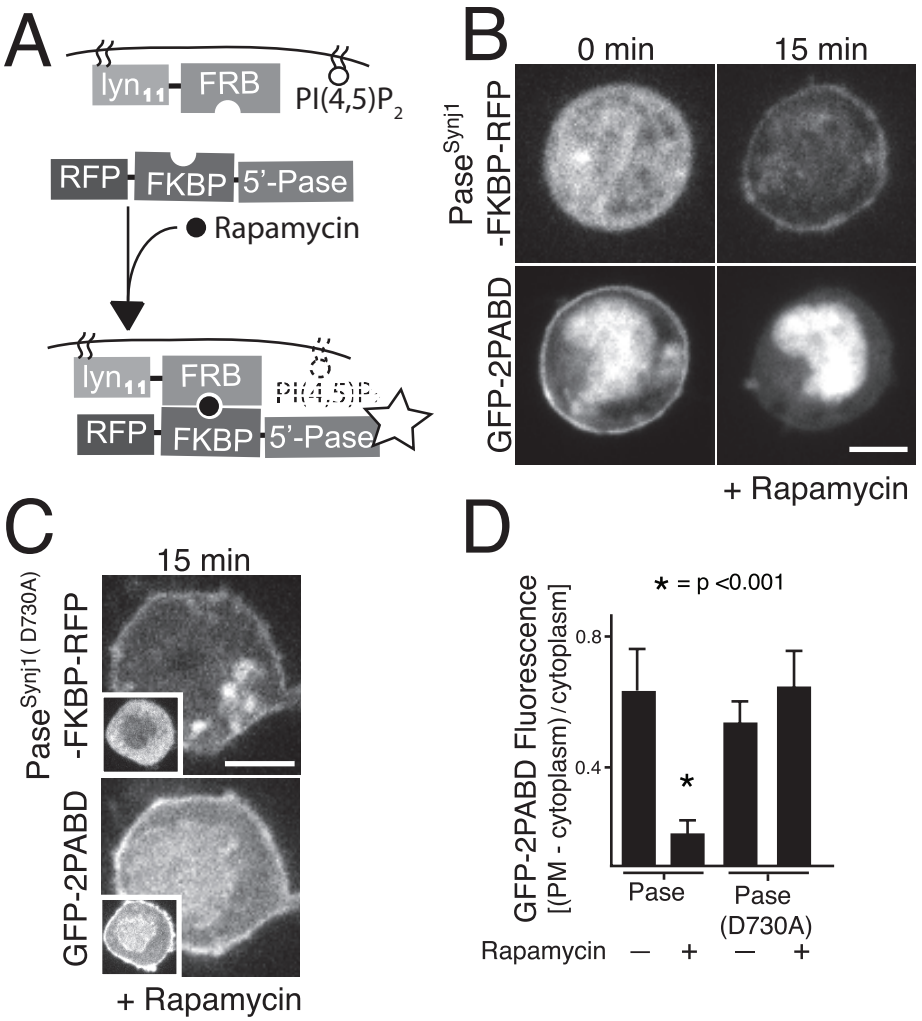

FIGURE 6: PtdIns(4,5)P_2 is required for plasmalemmal PA production. (A) Experimental strategy: RAW264.7 macrophages were transiently transfected with two complementary rapamycin-binding domains (LDR, which includes the membrane-targeting N-terminal sequence of Lyn and either active phosphatase-FKBP–RFP or phosphatase-dead-FKBP-RFP). Addition of rapamycin (black circle) induces translocation of the soluble FKBP domain–containing protein to the plasma membrane. The star indicates 5′-phosphatase activity at the plasma membrane. (B, C) RAW264.7 macrophages transiently cotransfected with LDR, GFP-2PABD, and either (B) active phosphatase ($Pase^{Synj1}$-FKBP-RFP) or (C) phosphatase-dead ($Pase^{Synj1(D730A)}$-FKBP-RFP). Confocal images were acquired immediately before (B, left, and C, inset) or 15 min after addition of 1 μM rapamycin. Scale bars, 5 μm. D) Quantification of plasmalemmal GFP-2PABD fluorescence relative to that in the cytosol for experiments depicted in B and C. Data are means ± SE of at least three individual experiments; a minimum of 20 cells were quantified per condition.

production is necessary for constitutive macropinocytosis in macrophages and iDCs.

DISCUSSION

Macrophages and iDCs are sentinels of the immune system, providing early defense against noxious agents. Their constant vigilance involves probing the environment for foreign antigens and invading microorganisms. Here we report that the actin polymerization that drives the membrane ruffling underlying such probing requires PA. Accordingly, macrophages and iDCs contain higher levels of plasmalemmal PA than those found in nonphagocytic cells, such as HeLa and HEK293.

PLD is considered to be an important source of PA. Remarkably, a variety of manipulations designed to impair PLD activity—addition of 1-butanol or FIPI, or the expression of dominant-negative alleles of PLD1 or PLD2—failed to reduce the level of plasmalemmal PA in phagocytes. These same conditions effectively suppressed PA levels induced by increased PLD activity in nonphagocytic cells (Shen *et al.*, 2001; Su *et al.*, 2009; see also Figure 2, B and D). Instead, our results indicate that phosphorylation of DAG is the primary source of the PA produced in the membrane of unstimulated macrophages and iDCs. The source of the DAG appears to be the hydrolysis of PtdIns(4,5)P_2 by PLC: not only do PLC inhibitors reduce the plasmalemmal PA, but so does the acute depletion of PtdIns(4,5)P_2 by specific, recruitable phosphatases. Furthermore, our results suggest that PLCβ but not PLCγ is responsible for the production of DAG. PLCβ isoforms are generally regulated by G protein–coupled receptors, and the observation that PA formation is susceptible to PTX, a G-protein antagonist, supports the involvement of β-type PLCs.

DAG released by PLCs is phosphorylated by DGK. Strikingly, phagocytes express all 10 known DGKs, and three of these were verified to be located at the plasma membrane. Although the redundancy of DGKs prevented identification of the specific family member(s) responsible for PA production, the effects of DGKi I clearly implied a role for these kinases. Two lines of evidence indicate that the effects of the inhibitor were specific: the delocalization of the GFP-2PABD induced by the inhibitor was reversed by addition of exogenous PA, and second, the reduction in PA was accompanied by an elevation in plasmalemmal DAG. The latter also implies that PA turns over rapidly; even in cells at rest, PtdIns(4,5)P_2 must be continuously hydrolyzed by PLC and the resulting DAG converted to PA. The inhibition of PLC could thus be expected to increase PtdIns(4,5)P_2. Accordingly, addition of PLC inhibitors is associated with increased cortical actin (Scott *et al.*, 2005), which is a sensitive index of PtdIns(4,5)P_2.

The accumulation of plasmalemmal PA seems to be essential for the constitutive ruffling of the membrane of phagocytes. This conclusion is supported directly by the inhibitory effects of DGKi I and indirectly by the inhibition caused by depletion of PtdIns(4,5)P_2 or inhibition of PLC. PA can modulate Rac activity and actin polymerization in a variety of synergistic ways (Zhang and Du, 2009): it contributes to the recruitment and activation of PtdIns(4)P5K (Roach *et al.*, 2012), stimulates the dissociation of Rac from its GDI (Abramovici *et al.*, 2009), and aids in the recruitment of Rac to the membrane (Stace and Ktistakis, 2006) and to its activation by GEFs (Nishikimi *et al.*, 2009). Yet, although necessary, PA is seemingly not sufficient to support membrane ruffling: overexpression of PLD2 induced production of PA in HeLa cells but did not elicit ruffling. Moreover, although PA was abundant throughout the plasma

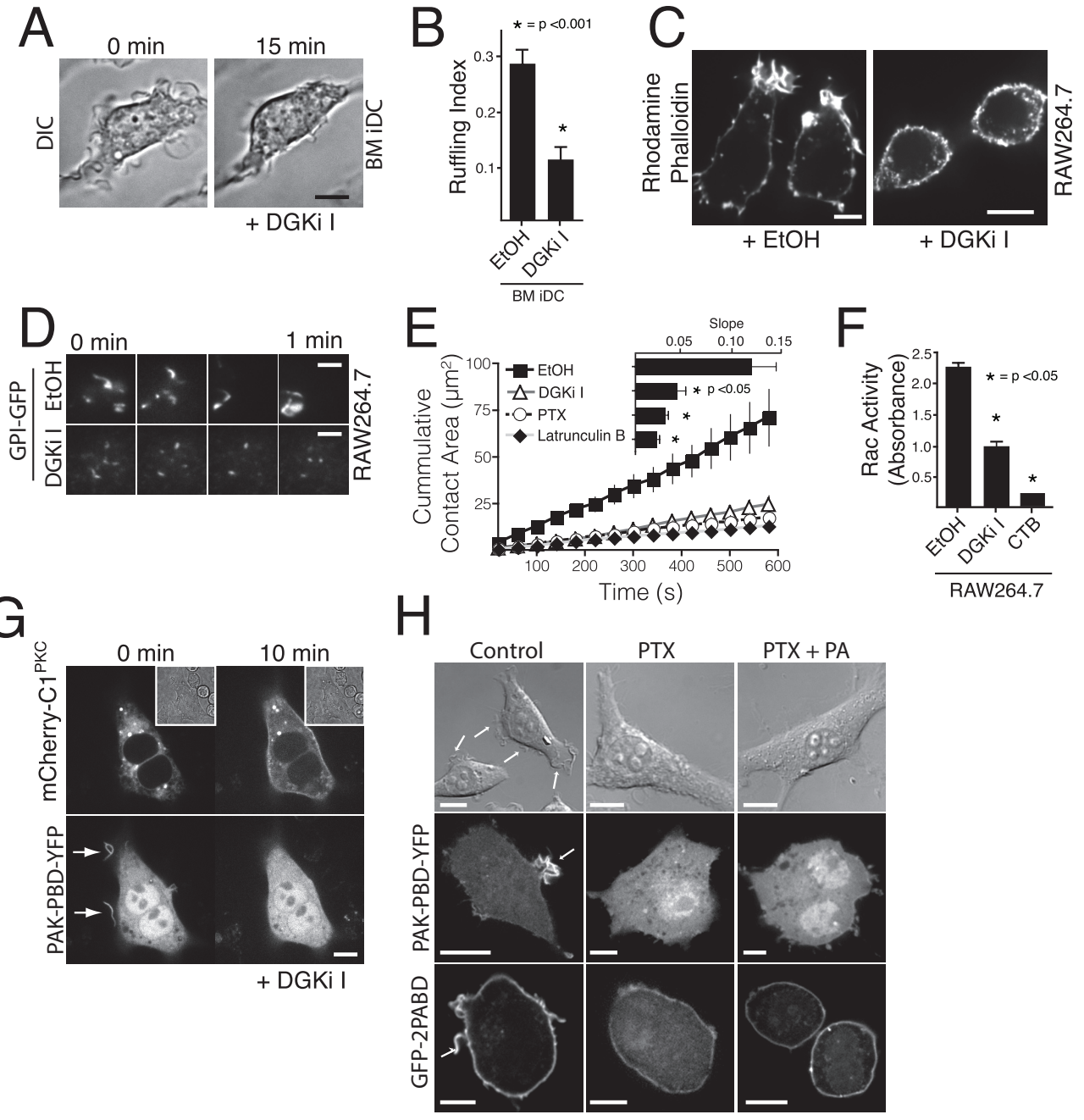

FIGURE 7: PA is required for steady-state ruffling. (A) Bone marrow–derived iDCs were imaged by differential interference contrast microscopy. Images were acquired immediately before and 15 min after treatment with 30 μM DGKi I. (B) Quantification of ruffling index of iDCs treated with either 30 μM DGKi I or solvent (ethanol [EtOH]; 0.3%) alone. Data are means ± SE of three individual experiments; a minimum of 30 cells were quantified per condition. (C) RAW264.7 macrophages treated with EtOH (left) or 30 μM DGKi I (right) were fixed, stained with rhodamine–phalloidin, and imaged by confocal microscopy. (D) RAW264.7 macrophages stably expressing GPI-linked GFP were pretreated with EtOH (top) or 30 μM DGKi I (bottom) for 20 min and allowed to settle onto bovine serum albumin–coated coverslips. Images were acquired at 40-s intervals by TIRF microscopy. (E) Cumulative fluorescence of the contact area of macrophages stably expressing GPI-linked GFP, integrated in the TIRF plane. Cells were treated with 30 μM DGKi I, 0.1 μg/mL PTX, 5 μM latrunculin B, or vehicle (EtOH) only, as indicated. Data are means ± SE of at least three individual experiments; a minimum of 10 cells were quantified per condition. Inset shows the mean slopes ± SE. (F) Quantification of active Rac detected in RAW264.7 cell lysates using an enzyme-linked immunosorbent assay. Cells were pretreated with 30 μM DGKi I for 20 min, 50 ng/ml *Clostridium* toxin B (CTB) for 1 h, or solvent (EtOH alone). Data are means ± SE of five individual experiments. (G) RAW264.7 cells transiently cotransfected with mCherry-$C1^{PKC}$ and PAK-PBD-YFP were imaged by confocal microscopy immediately before and 10 min after addition of 30 μM DGKi I. Insets show corresponding DIC images. (H) RAW264.7 macrophages were transiently transfected with either PAK-PBD-YFP or GFP-2PABD and incubated with 0.1 μg/ml PTX overnight (middle and right) or left otherwise untreated (left). Where indicated, 100 μM PA was added to the culture medium 20 min before analysis by differential interference contrast (top) or confocal (middle and bottom) microscopy. Scale bars, 5 μm.

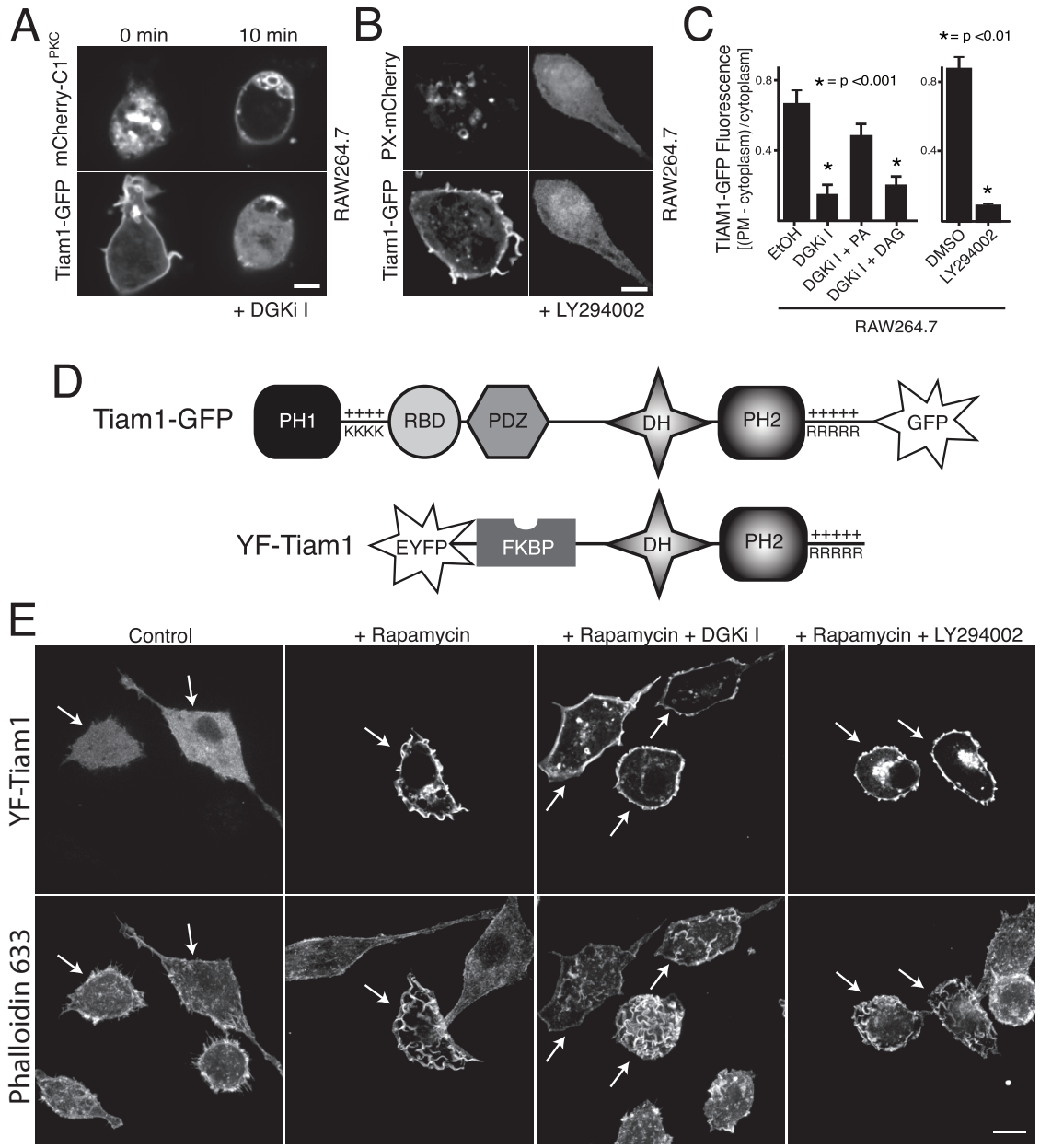

FIGURE 8: DGK- and PI3K-derived lipid signals are necessary for the constitutive association of TIAM1 with the phagocyte membrane. (A) RAW264.7 macrophages transiently cotransfected with mCherry-C1^{PKC} and TIAM1-GFP were imaged immediately before and 10 min after addition of 30 μM DGKi I. (B) RAW264.7 macrophages transiently transfected with either PX-mCherry or TIAM1-GFP were fixed immediately before or after exposure to 100 μM LY294002 and imaged by confocal microscopy. Scale bars, 5 μm. (C) Quantification of fluorescence at the plasma membrane of macrophages transiently transfected with TIAM1-GFP and treated with 0.3% ethanol, 30 μM DGKi I, 30 μM DGKi I plus 100 μM PA, 30 μM DGKi I plus 100 μM DAG, 0.1% DMSO, or 100 μM LY294002. Data are means ± SE of at least three individual experiments; a minimum of 30 cells were quantified per condition. (D) Modular domain architecture of TIAM1-GFP (top) and YF-TIAM1 (bottom). The former is composed of the full-length, wild-type sequence of TIAM1 fused to GFP, whereas the latter comprises only the tandem DH and PH domains of TIAM1 coupled to a rapamycin-binding domain (FKBP) and EYFP by a flexible linker. (E) RAW264.7 macrophages transfected with YF-TIAM1 were pretreated with DMSO (vehicle control), 1 μM rapamycin, or a combination of rapamycin and 30 μM DGKi I or rapamycin and 100 μM LY294002 before being fixed, permeabilized, and stained with Alexa 647–phalloidin. Top, single confocal sections that show redistribution of YF-TIAM1 upon exposure to rapamycin; bottom, *Z*-projections of multiple confocal sections that illustrate actin staining within extensive dorsal ruffles. Arrows point to macrophages transfected with YF-TIAM1. Scale bars, 10 μm.

membrane of macrophages and iDCs, ruffles formed only in localized areas. Clearly, other factors are permissive to the response. Of interest, aluminum fluoride, an activator of G proteins, promoted the recruitment of the PA probe to the membrane and the simultaneous formation of ruffle-like extensions in HeLa cells (Supplemental Movie S3). The GPCRs may reside sufficiently upstream in the signaling pathway, enabling them to enlist additional regulators of ruffling such as PI3K and/or Ras GTPases.

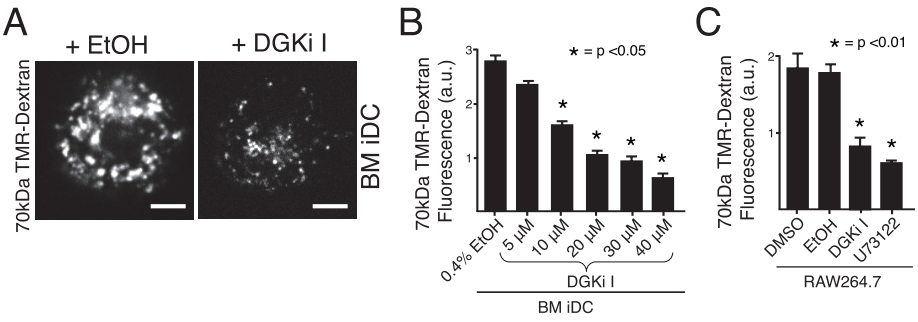

FIGURE 9: PA is required for macropinocytosis. (A) Bone marrow–derived iDCs pretreated with 0.3% EtOH (left) or 30 μM DGKi I (right) for 20 min were pulsed with tetramethylrhodamine (TMR)-dextran (70 KDa) for 1 h and imaged by confocal microscopy. Scale bars, 5 μm. (B, C) Quantification of the TMR-dextran fluorescence uptake. (B) iDCs were pretreated for 20 min with the indicated concentrations of DGKi I or with vehicle only and then incubated with TMR-dextran for 1 h, followed by imaging as described. Data are means ± SE of three individual experiments; a minimum of 100 cells were quantified per condition. (C) RAW264.7 macrophages were pretreated for 20 min with the indicated inhibitors or the corresponding solvents only and then incubated with TMR-Dextran for 1 h, followed by imaging as described. Data are means ± SE of three individual experiments; a minimum of 100 cells were quantified per condition.

Accordingly, we found that PtdIns(3,4,5)P_3 was detectable in the membrane of otherwise unstimulated macrophages and that its presence was also eliminated by PTX. Our data suggest that PtdIns(3,4,5)P_3, generated by the ongoing activity of a PTX-sensitive GPCR, plays at least two distinct roles in the genesis of membrane ruffling: it appears to be required for the recruitment to the membrane of TIAM1, which has an N-terminal PH domain known to bind PtdIns(3,4,5)P_3 (Figure 8; Ceccarelli *et al.*, 2007), and it most likely also contributes to the plasmalemmal recruitment and activation of PLCβ isoforms (Zhang *et al.*, 2006).

The formation of PA- and PtdIns(3,4,5)P_3-dependent ruffles on the surface of phagocytes fulfills two functions: they 1) underpin the formation of macropinosomes and 2) aid in probing the environment for phagocytic targets (Flannagan *et al.*, 2010), enabling the cells to dynamically extend their reach. However, the high basal level of PA may potentiate other key functions of myeloid cells. Neutrophil chemotaxis, which is similarly sensitive to PTX, requires membrane extension before integrin-mediated attachment to the substratum. In addition, because exocytosis is stimulated by PA in some cells (Zeniou-Meyer *et al.*, 2007), the secretion of cytokines and antimicrobial factors might also be facilitated in phagocytes. Finally, because PA can regulate mTOR activity (Fang *et al.*, 2001), it might influence the longevity of the phagocytes.

In summary, we found that the basal levels of PA vary greatly among cell types, being exceptionally high in phagocytes. This high level of PA, together with PtdIns(3,4,5)P_3, is critical for the continuous membrane ruffling that underlies the specialized function of macrophages and iDCs in immune surveillance.

MATERIALS AND METHODS

Cell culture, plasmids, transfection, and reagents

RAW264.7 and J774 macrophages, HeLa cells, and HEK293 cells were obtained from the American Type Culture Collection (Manassas, VA) and grown in RPMI medium supplemented with 5% heat-inactivated fetal bovine serum (Wisent, St. Bruno, Canada). Cells seeded on glass coverslips were transfected with FuGENE HD (Roche, Mississauga, Canada) according to the manufacturer's instructions. In brief, each well of a 12-well plate was treated with 1 μg of plasmid cDNA and 3 μl of FuGENE HD. Cells were used 24 h after transfection. Bone marrow–derived iDCs were generated from 6- to 8-wk-old female, wild-type C57BL/6 mice, according to Lutz *et al.* (1999). These primary cells were electroporated with 1 μg of plasmid cDNA using Ingenio electroporation solution (Mirus, Madison, WI) and used 8 h after electroporation with a Nucleofector I (Amaxa, Allendale, NJ). RAW264.7 macrophages stably expressing glycophosphatidylinositol (GPI)-linked GFP were described earlier (Flannagan *et al.*, 2010). The plasmid encoding GFP-2PABD consisted of GFP fused to a tandem repeat of the PA-binding domain of Spo20p reported before (Zeniou-Meyer *et al.*, 2007; Du and Frohman, 2009), which was modified by adding at the N-terminus a nuclear export sequence derived from protein kinase A inhibitor-α (unpublished data). Plasmids encoding HA-PLD1, HA-PLD2, HA-PLD1(K898R), and HA-PLD2(K758R) were from John Brumell (Hospital for Sick Children, Toronto, Canada). PLCβ1-GFP and PLCβ3-CFP were gifts from Theresa Filtz (Oregon State University, Corvallis, OR; Zhang *et al.*, 2006). The rapamycin heterodimerization constructs (LDR, phosphatase-FKBP-RFP, and phosphatase-dead-FKBP-RFP) were from Gilbert Di Paolo (Columbia University, New York, NY; Chang-Ileto *et al.*, 2011). The recruitable form of TIAM1 was obtained from Addgene (Cambridge, MA; plasmid 20154). PM-RFP, mCherry-C1 domain (PKCδ), PAK-PBD-YFP, PLCγ1-GFP, PLCγ2-GFP, TIAM1-GFP, GFP-R-pre, DGKα-GFP, DGKβ-GFP, DGKγ-GFP, DGKδ-GFP, DGKε-GFP, and DGKζ-GFP were described earlier (Shindo *et al.*, 2003; Yeung *et al.*, 2006; Flannagan *et al.*, 2010, 2012). PLCγ1 (2822) and PLCγ2 (3872) antibodies were from Cell Signaling (Boston, MA) and used to probe cells fixed in 4% paraformaldehyde (Electron Microscopy Sciences, Hatfield, PA). DGKi I (R59022; 30 μM in ethanol) and PTX (0.1 μg/ml overnight) were from Enzo Biochem (Farmingdale, NY). FIPI (750 nM), rapamycin (1 μM), U73122 (2 μM), and latrunculin B (5 μM) were from Sigma-Aldrich (St. Louis, MO). Insulin was from Eli Lilly (Toronto, Canada). Phorbol-12-myristate-13-acetate (0.1 μM) was from BioShop (Burlington, Canada). CTB (50 ng/ml in serum-free media for 1 h) was from Techlab (Blacksburg, VA). Rhodamine phalloidin and 70-kDa tetramethylrhodamine-dextran were from Molecular Probes (Eugene, OR). Ionomycin (0.1 μM) was from Calbiochem (San Diego, CA). PA (L-α-phosphatidic acid; 840074) and DAG (1,2-dioctanoyl-sn-glycerol; 800800) were from Avanti (Alabaster, AL); they were dried of chloroform under a stream of N_2 and made up to 100 μM with media containing 4 mg of essentially fatty acid–free albumin (Sigma-Aldrich). All other chemicals were from Sigma-Aldrich, including NaF (30 mM) and $AlCl_3$ (50 μM), which were added to media to produce AlF_3.

RT-PCR

To detect expression of the 10 DGKs and the two PLCβ isoforms of interest, we purified total cellular RNA from RAW264.7 macrophages with an RNeasy Mini Kit (Qiagen, Toronto, Canada), as instructed by the manufacturer. Purified total RNA was subsequently reverse transcribed and exponentially amplified using a OneStep RT-PCR kit (Qiagen). RNA was isolated from 8×10^5 RAW264.7 macrophages, and 1 μg of purified RNA was used as template for each reverse

transcription reaction. We used isoform-specific primers (see the following list) for cDNA generation and allowed the reaction to proceed for 30 min at 55°C. Reverse transcriptase was inactivated and Taq polymerase was activated by increasing the reaction temperature to 94°C for 4 min. PCR amplification was performed with the same isoform-specific primers as those used for reverse transcription at denaturing, annealing, and extension temperatures of 94 (30 s), 50 (30 s) and 68°C (1 min), respectively. The PCR cycle was iterated 33 times for every sample, excluding DGKβ, which underwent 40 cycles.

DGKα: forward, AAGGAAGCGTTGACAGCTGGAAGC; reverse, TTCTGGCCGGCCACCTTCTAGG

DGKβ: forward, CATCACCTACACCATGACAAACCAGG; reverse, CATTCGAGGTACTCTGCCACGTGC

DGKγ: forward, GCGCAACCAAGTGTTGCATGGT; reverse, AGACATTGGGCTCACTACTGCTGGC

DGKδ: forward, CAAGAGGAGGTACTTTAAGCTTCGAGGG; reverse, AATAGGTTGGCCGTGCATGGG

DGKε: forward, TTCTGCAGGCAGCAGTGTGGC; reverse, CATTACCTGTTCCCAGAGGTAAGACCG

DGKζ: forward, GACCAAGCGGCGCTTCCC; reverse, CAGCTGATGGCTACGATCTCCTTGC

DGKη: forward, GCAAACCAGCTCTTTCCAAAGGTGG; reverse, GCAGTTGTTTGTTGCCCTCACTGC

DGKθ: forward, AGTGCCTGAAGCAGGTGAAGACCC; reverse, AGGCAGTACCATGGAGCGTAGACG

DGKι: forward, GAGAATGCTGTGAATGGGGAGCAC; reverse, CCTTAATGATCCAGGTGGGCGG

DGKκ: forward, ACAATTGATCTGTCTCAAGTTGTTTTGGC; reverse, CCCTAGGGTCGCTCAGTGCCG

PLCβ1: forward, ACCTGCTGGCTCAGAACATGTCC; reverse, CCGCTCAGGTAGCGCATGAATCC

PLCβ3: forward, ACCTGGTGACCCTGCGTGTGG; reverse, CAGGACTCCAGCGCCGTCTCC

Analysis of phosphatidic acid by mass spectrometry

The lipids were extracted according to Folch *et al.* (1957) but omitting the salt. For quantification of the PA species, a mixture of internal standards was added at the one-phase stage of extraction. The extract was evaporated and redissolved in chloroform/methanol (1:2, vol/vol) and infused (6 µl/min) into a Micromass Quattro micro triple-quadrupole mass spectrometer (Waters, Milford, MA) operated as described previously (Hermansson *et al.*, 2005). The PA species were detected by scanning for precursors of *m/z* 153 (Brügger *et al.*, 1997) and then identified and quantified using LIMSA software (Haimi *et al.*, 2006).

Enzymatic assay and Rac enzyme-linked immunosorbent assay

PA content was measured enzymatically with a total PA assay kit (Abnova, Taipei City, Taiwan) according to manufacturer's instructions. In summary, for each sample, lipids were isolated from a confluent T25 flask using chloroform–methanol extraction. The cellular lipids were digested with lipase. Glycerol 3-phosphate, the product of PA digestion, was selectively oxidized by glycerol 3-phosphate oxidase to produce hydrogen peroxide. In the presence of peroxidase, the hydrogen peroxide levels were measured with Amplex red in a SpectraMax Gemini EM fluorescence microplate reader (Molecular Devices, Sunnyvale, CA). Before chloroform–methanol extraction, the protein content of each sample was measured with a bicinchoninic acid assay (Thermo Scientific, Rockford, IL).

Rac activity was measured with a G-LISA kit against all three Rac isoforms (Cytoskeleton, Denver, CO) according to manufacturer's instructions. In short, total cell lysates were equalized based on their protein concentrations and seeded on a well that bound active Rac. Cellular debris was washed away, and the bound Rac was probed with an anti-Rac antibody, followed by secondary antibody tagged with horseradish peroxidase. The signal was measured with a SpectraMax 190 absorbance microplate reader (Molecular Devices, Sunnyvale, CA) at 490 nm after incubation of the well with a detection reagent.

Microscopy and analysis

Cells on coverslips were transferred into 4-(2-hydroxyethyl)-1-piperazineethanesulfonic acid–buffered RPMI medium (Wisent). Differential interference contrast microscopy was performed on a DMIRE2 microscope (Leica, Solms, Germany) with Volocity (version 4.3.2; PerkinElmer, Waltham, MA). TIRF images were taken with a cell^TIRF system (Olympus, Tokyo, Japan) equipped with a 50-mW, 491-nm laser and a 150×/1.45 numerical aperture (NA) objective and operated by Volocity. All other images were captured using a spinning-disk confocal microscopy system (Quorum, Guelph, Canada) with a 63×/1.4 NA objective on an Axiovert 200M microscope (Zeiss, Toronto, Canada). Images were captured at 37°C with a back-thinned electron-multiplier ImagEM C9100-13 camera (Hamamatsu, Hamamatsu City, Japan) and Volocity.

Images were analyzed using Volocity (version 6.0.1) and ImageJ (National Institutes of Health, Bethesda, MD). The ruffling index was calculated according to previous methodology (Araki *et al.*, 1996). Statistical tests were performed in SPSS 17 (IBM, Armonk, NY), using the Kruskal–Wallis test with a Dunn's correction for multiple comparisons where necessary. TIRF data were analyzed using polynomial fitting in Prism (GraphPad, La Jolla, CA).

ACKNOWLEDGMENTS

M.B. is funded by an M.D./Ph.D. Scholarship from the Canadian Institutes of Health Research. This work was supported by Canadian Institutes of Health Research Grants MOP7075 and MOP93634. S.G. is the current holder of the Pitblado Chair in Cell Biology at the Hospital for Sick Children.

REFERENCES

Abramovici H, Mojtabaie P, Parks RRJ, Zhong X-P, Koretzky GA, Topham MK, Gee SH (2009). Diacylglycerol kinase ζ regulates actin cytoskeleton reorganization through dissociation of Rac1 from RhoGDI. Mol Biol Cell 20, 2049–2059.

Andreyev AY *et al.* (2010). Subcellular organelle lipidomics in TLR-4-activated macrophages. J Lipid Res 51, 2785–2797.

Araki N, Johnson MT, Swanson JA (1996). A role for phosphoinositide 3-kinase in the completion of macropinocytosis and phagocytosis by macrophages. J Cell Biol 135, 1249–1260.

Bohdanowicz M, Grinstein S (2013). Role of phospholipids in endocytosis, phagocytosis, and macropinocytosis. Physiol Rev 93, 69–106.

Brügger B, Erben G, Sandhoff R, Wieland FT, Lehmann WD (1997). Quantitative analysis of biological membrane lipids at the low picomole level by nano-electrospray ionization tandem mass spectrometry. Proc Natl Acad Sci USA 94, 2339–2344.

Bunney TD, Katan M (2011). PLC regulation: emerging pictures for molecular mechanisms. Trends Biochem Sci 36, 88–96.

Ceccarelli DFJ, Blasutig IM, Goudreault M, Li Z, Ruston J, Pawson T, Sicheri F (2007). Non-canonical interaction of phosphoinositides with pleckstrin homology domains of Tiam1 and ArhGAP9. J Biol Chem 282, 13864–13874.

Chang-Ileto B, Frere SG, Chan RB, Voronov SV, Roux A, Di Paolo G (2011). Synaptojanin 1-mediated PI(4,5)P2 hydrolysis is modulated by membrane curvature and facilitates membrane fission. Dev Cell 20, 206–218.

Du G, Altshuller YM, Vitale N, Huang P, Chasserot-Golaz S, Morris AJ, Bader M-F, Frohman MA (2003). Regulation of phospholipase D1 subcellular cycling through coordination of multiple membrane association motifs. J Cell Biol 162, 305–315.

Du G, Frohman MA (2009). A lipid-signaled myosin phosphatase surge disperses cortical contractile force early in cell spreading. Mol Biol Cell 20, 200–208.

Fang Y, Vilella-Bach M, Bachmann R, Flanigan A, Chen J (2001). Phosphatidic acid-mediated mitogenic activation of mTOR signaling. Science 294, 1942–1945.

Flannagan RS, Harrison RE, Yip CM, Jaqaman K, Grinstein S (2010). Dynamic macrophage "probing" is required for the efficient capture of phagocytic targets. J Cell Biol 191, 1205–1218.

Flannagan RS, Jaumouillé V, Huynh KK, Plumb JD, Downey GP, Valvano MA, Grinstein S (2012). *Burkholderia cenocepacia* disrupts host cell actin cytoskeleton by inactivating Rac and Cdc42. Cell Microbiol 14, 239–254.

Folch J, Lees M, Sloane Stanley GH (1957). A simple method for the isolation and purification of total lipides from animal tissues. J Biol Chem 226, 497–509.

Haimi P, Uphoff A, Hermansson M, Somerharju P (2006). Software tools for analysis of mass spectrometric lipidome data. Analyt Chem 78, 8324–8331.

Hermansson M, Uphoff A, Käkelä R, Somerharju P (2005). Automated quantitative analysis of complex lipidomes by liquid chromatography/mass spectrometry. Analyt Chem 77, 2166–2175.

Inoue T, Heo WD, Grimley JS, Wandless TJ, Meyer T (2005). An inducible translocation strategy to rapidly activate and inhibit small GTPase signaling pathways. Nat Methods 2, 415–418.

Kassas N, Tryoen-Tóth P, Corrotte M, Thahouly T, Bader M-F, Grant NJ, Vitale N (2012). Genetically encoded probes for phosphatidic Acid. Methods Cell Biol 108, 445–459.

Lutz MB, Kukutsch N, Ogilvie AL, Rössner S, Koch F, Romani N, Schuler G (1999). An advanced culture method for generating large quantities of highly pure dendritic cells from mouse bone marrow. J Immunol Methods 223, 77–92.

Mizrahi A, Molshanski-Mor S, Weinbaum C, Zheng Y, Hirshberg M, Pick E (2005). Activation of the phagocyte NADPH oxidase by Rac guanine nucleotide exchange factors in conjunction with ATP and nucleoside diphosphate kinase. J Biol Chem 280, 3802–3811.

Morita S-ya, Ueda K, Kitagawa S (2009). Enzymatic measurement of phosphatidic acid in cultured cells. J Lipid Res 50, 1945–1952.

Nakanishi H, de los Santos P, Neiman AM (2004). Positive and negative regulation of a SNARE protein by control of intracellular localization. Mol Biol Cell 15, 1802–1815.

Nishikimi A *et al*. (2009). Sequential regulation of DOCK2 dynamics by two phospholipids during neutrophil chemotaxis. Science 324, 384–387.

Rizzo MA, Shome K, Watkins SC, Romero G (2000). The recruitment of Raf-1 to membranes is mediated by direct interaction with phosphatidic acid and is independent of association with Ras. J Biol Chem 275, 23911–23918.

Roach AN, Wang Z, Wu P, Zhang F, Chan RB, Yonekubo Y, Di Paolo G, Gorfe AA, Du G (2012). Phosphatidic acid regulation of PIPKI is critical for actin cytoskeletal reorganization. J Lipid Res 53, 2598–2609.

Sakane F, Imai S-I, Kai M, Yasuda S, Kanoh H (2007). Diacylglycerol kinases: why so many of them. Biochim Biophys Acta 1771, 793–806.

Scott CC, Dobson W, Botelho RJ, Coady-Osberg N, Chavrier P, Knecht DA, Heath C, Stahl P, Grinstein S (2005). Phosphatidylinositol-4,5-bisphosphate hydrolysis directs actin remodeling during phagocytosis. J Cell Biol 169, 139–149.

Shen Y, Xu L, Foster DA (2001). Role for phospholipase D in receptor-mediated endocytosis. Mol Cell Biol 21, 595–602.

Shindo M, Irie K, Masuda A, Ohigashi H, Shirai Y, Miyasaka K, Saito N (2003). Synthesis and phorbol ester binding of the cysteine-rich domains of diacylglycerol kinase (DGK) isozymes. DGKgamma and DGKbeta are new targets of tumor-promoting phorbol esters. J Biol Chem 278, 18448–18454.

Srinivasan S, Wang F, Glavas S, Ott A, Hofmann F, Aktories K, Kalman D, Bourne HR (2003). Rac and Cdc42 play distinct roles in regulating PI(3,4,5)P3 and polarity during neutrophil chemotaxis. J Cell Biol 160, 375–385.

Stace CL, Ktistakis NT (2006). Phosphatidic acid- and phosphatidylserine-binding proteins. Biochim Biophys Acta 1761, 913–926.

Su W, Yeku O, Olepu S, Genna A, Park J-S, Ren H, Du G, Gelb MH, Morris AJ, Frohman MA (2009). 5-Fluoro-2-indolyl des-chlorohalopemide (FIPI), a phospholipase D pharmacological inhibitor that alters cell spreading and inhibits chemotaxis. Mol Pharm 75, 437–446.

Vieira OV, Botelho RJ, Rameh L, Brachmann SM, Matsuo T, Davidson HW, Schreiber A, Backer JM, Cantley LC, Grinstein S (2001). Distinct roles of class I and class III phosphatidylinositol 3-kinases in phagosome formation and maturation. J Cell Biol 155, 19–25.

Wang Z *et al*. (2008). Phospholipase C beta3 deficiency leads to macrophage hypersensitivity to apoptotic induction and reduction of atherosclerosis in mice. J Clin Invest 118, 195–204.

West MA, Prescott AR, Eskelinen EL, Ridley AJ, Watts C (2000). Rac is required for constitutive macropinocytosis by dendritic cells but does not control its downregulation. Curr Biol 10, 839–848.

Yeung T, Grinstein S (2007). Lipid signaling and the modulation of surface charge during phagocytosis. Immunol Rev 219, 17–36.

Yeung T, Terebiznik M, Yu L, Silvius J, Abidi WM, Philips M, Levine T, Kapus A, Grinstein S (2006). Receptor activation alters inner surface potential during phagocytosis. Science 313, 347–351.

Zeniou-Meyer M *et al*. (2007). Phospholipase D1 production of phosphatidic acid at the plasma membrane promotes exocytosis of large dense-core granules at a late stage. J Biol Chem 282, 21746–21757.

Zhang L, Mao YS, Janmey PA, Yin HL (2012). Phosphatidylinositol 4, 5 bisphosphate and the actin cytoskeleton. Subcell Biochem 59, 177–215.

Zhang Y, Du G (2009). Phosphatidic acid signaling regulation of Ras superfamily of small guanosine triphosphatases. Biochim Biophys Acta 1791, 850–855.

Zhang Y, Kwon SH, Vogel WK, Filtz TM (2009). PI(3,4,5)P3 potentiates phospholipase C-beta activity. J Recept Signal Transduct Res 29, 52–62.

Zhang Y, Vogel WK, McCullar JS, Greenwood JA, Filtz TM (2006). Phospholipase C-beta3 and -beta1 form homodimers, but not heterodimers, through catalytic and carboxyl-terminal domains. Mol Pharmacol 70, 860–868.